Quantitative Image Based Tumour Vessel Radius Analysis

Wang Po[1]
wangpo@robots.ox.ac.uk
Sir Michael Brady[1]
jmb@robots.ox.ac.uk
Cat Kelly[2]
ckelly@rob.ox.ac.uk

[1] Wolfson Medical Vision Lab
University of Oxford
Oxford, UK

[2] Gray Institute for Radiation Oncology
University of Oxford,
Oxford, UK

Abstract

Abnormal vascular structure has been identified as a major characteristic of tumours. In this paper, we compare the vascular radii change due to the treatment of inhibitors in the RAS-PI3K AKT pathway. We contend that the distribution of vessel radii is more suitably be modelled as a gamma distribution than the log-normal distribution proposed in previous research. Based on this assumption, we conclude that all the inhibitors tested increased tumour vessel radius at the 0.05 significance level.

1 Introduction

Tumour vasculature is often substantially less efficient in delivering oxygen and other nutrients. The malformation of tumour vasculature is believed to be one of the causes that lead to tumour hypoxia and necrosis. Some drugs have been developed to re-normalize the tumour vasculature in order to improve the oxgygenation in tumours and to yield optimal responses for chemotherapies and/or radiotherapies. RAS-PI3K-AKT is an important tumour angiogenesis signal pathway, and drugs have been developed specifically to inhibit this pathway. In this paper, we compare tumour vessel radii against those treated with FTI,IRessa,NFV and PI103. We conclude that these drugs can increase tumour vessel radii, so improving tumour vessel capacity in oxygen and nutrient delivery.

2 Method

Mice bearing human tumour xenografts were treated with four drugs, FTI (a farnesyl transferase inhibitor), IRessa, NFV (nelfinavir) and PI103 for 5 days. Microscopy images were obtained by Dr.Naseer Qayum following the protocol presented in [7]. Microscopic images were segmented using hysteresis thresholding and the vessel skeletons obtained through modified thinning operations. At each skeleton voxel, we sample the local vessel volume in either the XY, XZ or YZ plane. One projected image is shown in Fig.1.

We extracted the connected region containing the centre pixel of the projected image. (Because this is the projected region of the local vessel volume at the skeleton voxel) We

(a) Sample projected image

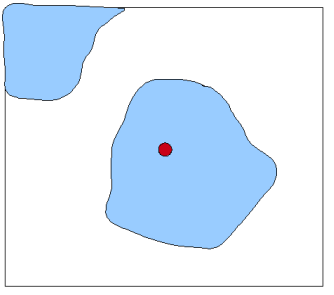

(b) Radius is calculated in the center connected region, assuming it as a circle

Figure 1: Sample projected image and illustration of radius calculation

measured the projected image area and calculated the orthogonal projection area using the projection angle. As observed from the projected image, the vessel's shape can be far from being circular. We assume that the *ex vivo* environment and imperfectness in histochemical staining could be the cause of the non-cylindrical vessel appearance. However, we contend that the blood vessel should be approximately cylindrical since *in vivo* vascular pumping and pressure would lead naturally to this shape. To simulate the *in vivo* environment, we assumed circular shape and calculated the vessel radius as Eq.1

$$r = \sqrt{\frac{S}{\pi}} \tag{1}$$

where S is the vessel orthogonal section area at each skeleton voxel.

3 Result

3.1 Data description

We processed 3 to 5 microscopic images for each drug group. Fig.2 shows the average and spread descriptor of vessel radii in drug treated and untreated tumour vasculature.

From the average radius values shown in Fig.2, we hypothesize that the radii of drug treated vessels are larger than for untreated tumour vessels. To test this hypothesis, we have first to determine the distribution of vessel radii.

3.2 Distribution assumption

Several researchers have modelled the radius distribution as log-normal [1]. However, we have found that the logarithms of vessel radii fail to pass the standard normality test (Lilliefors,$p<0.05$). We summarize the skewness and kurtosis of the radii logarithms' distribution in Tab.1.

We contend that the distribution of vessel radii might more suitably be modelled as a gamma distribution. Fig.3 compares the shape of best fitting lognormal distribution (red) and the best fitting gamma distribution (blue) and the data distribution. The parameters of

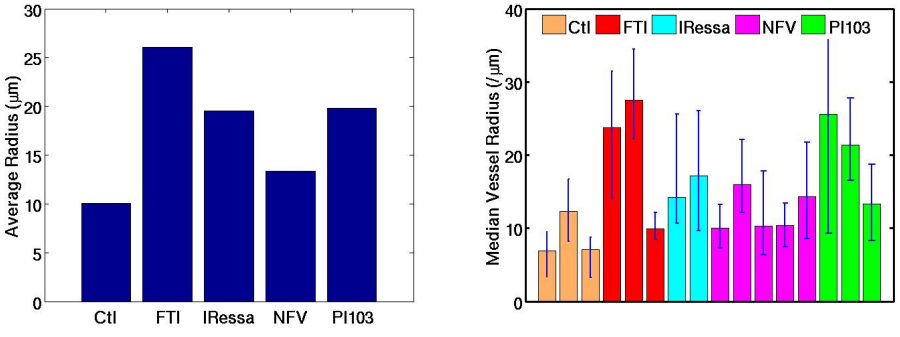

(a) Average of each drug group

(b) Average of each image

Figure 2: Comparison of average vessel radius of each vessel structure. In the group average (left), we used the mean value as a measure of the average vessel radius of each drug treated sample; in the image average (right), we used the median value (2nd quartile) as a measure of the average vessel radius of each vessel image and used the first and third quartile values as a measure of spread.

	skewness	kurtosis
Control	-1.3992	7.1228
FTI treated	-1.9553	9.4393
IRessa treated	-1.1537	5.5151
NFV treated	-1.0197	5.2441
PI103 treated	-1.2013	5.3625

Table 1: skewness and kurtosis of the logarithms of radii as compared to the normal distribution.

best fitting lognormal and gamma distributions were determined using maximum likelihood estimation.

To compare quantitatively the fits of the log-normal and gamma distributions to the observed data, we first calculated the Kaplan-Meier estimate of the cumulative distribution function (cdf) of the observed data. Since this cumulative distribution is derived directly from the observed data, it is also called the empirical cdf. This cdf serves as ground-truth of observed data's distribution characteristics. Fig.4 summarizes the data cumulative distribution function plots and the best fitted gamma and lognormal cumulated distribution function plots.

To evaluate the discrepancy between the fitting distribution and the ground truth, we calculated the sum of squared errors (RSS) of the log-normal and gamma fits respectively; they are listed in Tab.2

	Sample Size	RSS_{logn}	RSS_{gamma}
Control	886	1.4894	0.3510
FTI treated	691	4.7723	2.3878
IRessa treated	2030	2.51	0.2936
NFV treated	3848	5.0204	0.8878
PI103 treated	2361	4.8343	0.7218

Table 2: Total RSS of log-normal fitting cdf and gamma fitting cdf compared with the data's empirical cdf.

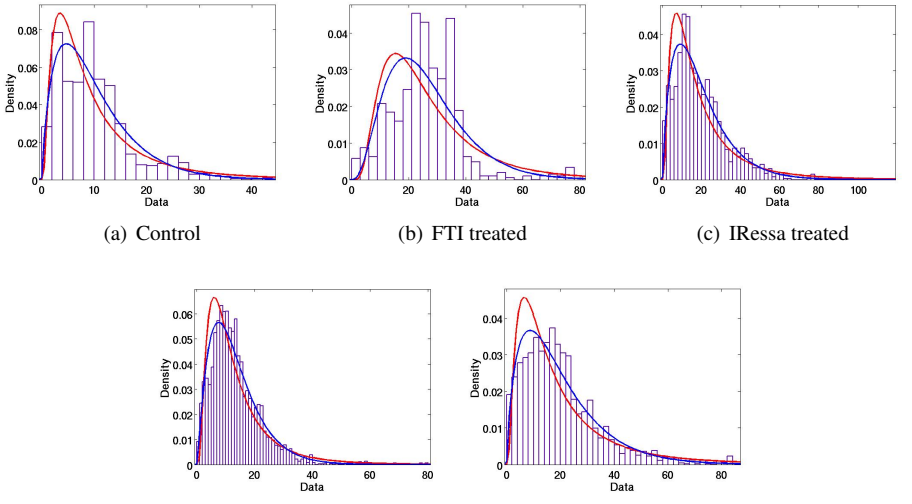

(a) Control (b) FTI treated (c) IRessa treated

(d) NFV treated (e) PI103 treated

Figure 3: Comparison of the log-normal fitting (red) and gamma fitting (blue) of the radius distribution.

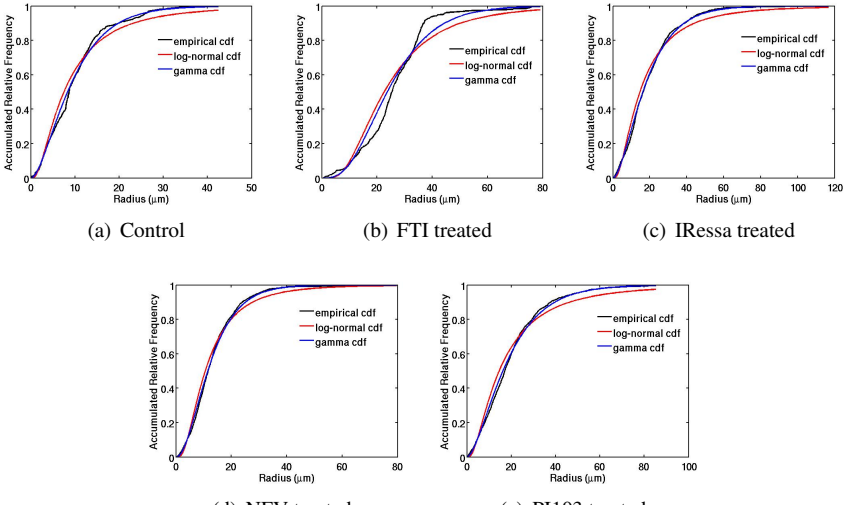

(a) Control (b) FTI treated (c) IRessa treated

(d) NFV treated (e) PI103 treated

Figure 4: Comparison of empirical cdf (black) and log-normal fitting distribution cdf (red) and gamma fitting distribution cdf (blue).

From Tab.2, the total RSS of the gamma fit is considerably smaller than for the log-normal fit. However, since the total RSS is related to the sample size, the total RSSs between different samples are not directly comparable. Because the gamma fit distribution cdf has smaller total RSS than the corresponding cdf of log-normal fitting, we contend that the vessel radius is better modeled as a gamma distribution.

3.3 Statistical inference

We followed the inference procedure proposed by [3]. Essentially, suppose μ_1 and μ_2 are the population mean values of two gamma distributed samples; then the approximate α-level test of H_0: $\mu_1 = \mu_2$ against H_a: $\mu_2 > \mu_1$ is provided by rejecting H_0 if the inequality (Eq.2) holds:

$$\frac{\bar{S}_1}{\bar{S}_2} < F_\beta(2n_1E(k_1), 2n_2E(k_2)) \tag{2}$$

where β is the adjusted significance level, $E(k_1)$,$E(k_2)$ are the gamma distribution scale parameter expectations, which were determined by the formula provided by [3]. We estimated the corresponding β values for each α using Monte Carlo simulations for different combinations of n_1,n_2,k_1,k_2 and α which can be found in [3].

We conducted the statistical inference and found that all drug treated tumour vessels have larger average radius than the untreated tumour vessels (p<0.05). We further analyzed the relationship between each drug treated vessels and found $R_{FTI} > R_{PI103}, R_{IRessa} > R_{NFV}$ (p<0.05).

4 Conclusion

The statistical analysis shows that each of the RAS-PI3K pathway inhibitors have significant effects in increasing the tumour vessel radii. The distribution assumption may provide some insights into the angiogenesis process. Since gamma distribution is the sum distribution of exponential distributions, it is primarily used to model the time elapsed for an upcoming event. In the angiogenesis scenario, the growth of blood vessels is affected by concentration of various signal molecules. The waiting time can be modelled as the distance of vessel loci to the source of these signal molecules. Indeed, tumour angiogenesis is essentially a dynamic process, whereby destruction and assembly processes reach dynamic equilibrium. The vessel radii can then be viewed as an indicator of the equilibrium states. Inhibition of the destruction process will lead to larger vessel radii.

To research further quantitatively tumour vessel formation and drug inhibition processes, it would be intriguing to develop a mathematical model. Validating this model by observed vessel structural change would yield insights into the mechanism of signal regulation in tumour angiogenesis.

References

[1] MA Konerding, E. Fait, and A. Gaumann. 3D microvascular architecture of precancerous lesions and invasive carcinomas of the colon. *British journal of cancer*, 84 (10):1354–1362, 2001.

[2] N. Qayum, R.J. Muschel, J.H. Im, L. Balathasan, C.J. Koch, S. Patel, W.G. McKenna, and E.J. Bernhard. Tumor Vascular Changes Mediated by Inhibition of Oncogenic Signaling. *Cancer Research*, 69(15):6347, 2009.

[3] W.K. Shiue, L.J. Bain, and M. Engelhardt. Test of equal gamma-distribution means with unknown and unequal shape parameters. *Technometrics*, 30(2):169–174, 1988.